Natural convection heat transfer in elliptic annuli with different aspect ratios

E.I. Eid
Mech. Ind. Dept., Faculty of Industrial Education, Suez Canal University, Suez, Egypt

In this paper, natural convection heat transfer in elliptic annuli with different aspect ratios was studied experimentally and numerically. Four test specimens having elliptic annuli cross sections with different aspect ratios of 0.25, 0.5, 0.75 and 1 and an annulus diameter ratio of 2 were tested experimentally. The specimens were tested experimentally at different orientation modes. In order to verify the experimental results, a mathematical model in two dimensional coordinates for two concentric cylinders was done. The model was solved numerically using the FLUENT CFD package. The predicted streamlines and isotherm contours were used to show the fluid movement and the temperature gradient within the annulus. The results show that the rotation of the elliptic annuli with small aspect ratio by a right angle whenever the specimens are horizontal or inclined improves the free convective heat transfer characteristics. The numerical predictions show that the annulus diameter ratio has more significant effect on the results rather than the orientation mode. The experimental results were fitted to deduce empirical correlations. A comparison between experimental data and numerical predictions of the present work was done. Another comparison among the results of the present work and that from the previous works was also done.

في هذا البحث يتم دراسة انتقال الحرارة بالحمل الطبيعي في مقطع حلقي على شكل قطع ناقص ذو نسبة محورين متغيرة عمليا وعدديا. تم تصنيع عدد أربعة عينات كل منهم عبارة عن اسطوانتين متحدتي المركز مقطع كل منهما قطع ناقص بنسب محورين متغيرة هم ٠,٢٥، ٠,٥٠، ٠,٧٥، ١ ونسبة القطر للقطاعات الحلقية الأربعة ثابتة وتساوى ٢. تم اختبار العينات الأربعة في أوضاع مختلفة (رأسيا - أفقيا بدون دوران المحور الأكبر - أفقيا مع دوران المحور الأكبر بزاوية ٤٥ درجة - أفقيا مع دوران المحور الأكبر ٩٠ درجة - مائلا بدون دوران المحور الأكبر - مائلا مع دوران المحور الأكبر بزاوية ٩٠ درجة). تم عمل محاكاة نظرية للدراسة عن طريق وضع المعادلات الحاكمة لسريان تطابقي انضغاطي مستقر ثنائي البعد عبر مقطع حلقي أفقي وآخر رأسي وقد تم حل المعادلات عدديا باستخدام برنامج معد خصيصا للحل العددي لديناميكا المائع. وقد تبين من خلال هذا البحث أن انتقال الحرارة بالحمل الطبيعي يمكن تحسينه في المقطع الحلقي على شكل قطع ناقص ذو نسبة محورين منخفضة في الوضع الأفقي مع دوران المحور الأكبر بزاوية ٩٠ درجة وكذا في الوضع المائل عنه في حالة المقطع الحلقي الدائري في ذات الوضع. كما خلصت المحاكاة النظرية إلى بيان تأثير نسبة القطر للمقطع الحلقي على الحمل الطبيعي بداخله. هذا وقد تم عمل معادلات وضعية لتوصيف النتائج المعملية. تم عقد مقارنة بين نتائج البحث العملية والنظرية وكذا عقد مقارنة أخرى بين نتائج البحث وسابقيه عند نفس الظروف للتأكد من قبول النتائج ووجد توافق كمي وكيفي ملحوظ في مدى المقارنة.

Keywords: Natural convection, Heat transfer, Elliptic annuli, Aspect ratio, Orientation mode, Modeling and CFD packages

1. Introduction

Natural convection heat transfer in the annuli between two circular or elliptic cylinders is one of the important topics in the engineering applications. Recently, many researches are conducted with this subject due to its wide range of applications. Applications are found in energy conversion, storage systems, transmission systems, solar collectors, nuclear reactors and phase change materials. The natural convection heat transfer in horizontal circular concentric annuli was studied experimentally and numerically over a wide range of Rayleigh number, [1]. Experimental work was conducted with the visualization of the flow pattern. The numerical predications for stream and temperature contours were compared with experimental results to determine the dominant flow pattern. An experimental study was performed to investigate the natural convection heat transfer

of helium between two horizontal isothermal concentric circular cylinders at cryogenic temperatures, [2]. The experimental results were correlated for $6\times10^6<Ra<2\times10^9$, Pr= 0.688, diameter ratio = 3.36 and an expansion number ($\beta\ \Delta T$) varied from 0.2 to 1. The transient natural convection between horizontal concentric circular cylinders was studied experimentally and numerically, [3]. Photographs were taken for successive positions of the plume of the heated fluid. A finite-domain method was used to simulate the phenomena numerically. The comparison between the predictions and experiments shows fairly good qualitative and quantitative agreement. The natural convection heat transfer in horizontal circular annuli with a constant heat flux at inner surface and a constant temperature at outer one was studied experimentally and numerically, [4]. The numerical solution was done for $1.8 \le do/di \le 15$ and Pr = 0.7, 5 and 100. A comparison between the numerical and experimental work was done at $74 < Pr < 173$ and at a diameter ratio of 11. The results gave the critical values of Rayleigh number at which the conduction regime changes to convection. The heat transfer from a plate-fin having one and two row arrangements of tubes with elliptic cross section were studied experimentally, [5]. The results were compared with those of circular tubes and it was found that the elliptic tubes have higher fin efficiency than that of the circular tubes. The natural convection heat transfer in a horizontal eccentric annulus between a square outer cylinder and a heated inner circular cylinder was studied numerically, [6]. The numerical solution was performed at different values of Rayleigh number, eccentric distance and angular position of the inner cylinder. The results show that the angular position of the inner cylinder and the eccentricity are having a significant effect on the plume inclination. The mixed convection heat transfer from an inclined elliptic tube placed in a fluctuating free stream was studied numerically, [7]. The effect of both amplitude and frequency of fluctuations on heat transfer was clarified for $50 < Re < 500$ an inclination angle of 30^o and an aspect ratio of 0.5. It was found that, the average Nusselt number increases with increasing the amplitude and decreasing the frequency of the fluctuations. The enhancement of natural convection from horizontal cylinders by using shrouding strips was studied experimentally, [8]. The number of strips, strip height, gap distance and the inclination angle of the strips were changed to achieve an enhancement up to 44.3 % rather than the smooth cylinders. The natural convection heat transfer in horizontal and inclined concentric circular annuli was studied experimentally and numerically, [9]. The results were presented for two diameter ratios of 1.63 and 2.57 and angles of inclination 0, 30, 45 and 60^o. Rayleigh number, based on the annulus gap width was varied from 1700 to 40000. The experimental and numerical results were in a close agreement for the horizontal orientation mode.

The aforementioned survey indicates that most researches studied the natural convection heat transfer through circular annuli. In the present work, natural convection heat transfer in concentric elliptic annuli was investigated experimentally and numerically. The effect of the aspect ratio of the elliptic section, which is the ratio between minor and major axes lengths, the effect of different orientation modes of the elliptic annuli and the effect of the diameter ratio of the annulus on the natural convective heat transfer were investigated. The present contribution presents a simulation of the problem as a mathematical model which was solved numerically using the FLUENT CFD package to verify the reliability of both experiments and numerical model. Empirical correlations were deduced to generalize the experimental results. A comparison among the present work and the previous works in the literature was done.

2. Experimental setup

The experimental setup shown in fig. 1 consists of the test specimen, an electric heater, a voltmeter, an ammeter, an altering variance unit, certain number of calibrated K-type thermocouples and a temperature indicator. The test specimens are four pairs of concentric cylinders as shown in fig. 2, one has circular cross section and three ones have

elliptic cross sections. The main dimensions of the test specimens are given in table 1. The specimens have an equal length of 900 mm. The circumferences of the inner circle of the specimen No. I and the inner ellipses of the three elliptic specimens No. II, III and IV, are equal, as well as the circumferences of the outer ones.

From table 1, it is clear that the specimens have different aspect ratios of 0.25, 0.5, 0.75 and 1. The specimens were manufactured from aluminum by using the wire-cut JSEDM machining, [10]. The inner cylinder was internally heated by an electric nickel-chrome heater which was wrapped about a bakelite rod. An electric insulation tape was wrapped about the heater and the space between the heater and the inner surface of the inner cylinder was partially filled with sand to avoid the convection currents. Thirty K-type thermocouples were used to measure the local surface temperatures of the outer surface of the inner cylinder in both circumferential and axial directions, [11]. They were positioned and arranged at equal angles on five cross sections; one at the mid-section, two ones over the mid-section and two ones under the mid-section. The five sections are at an equal axial distance of 15 cm. Other thirty thermocouples were arranged and positioned at the inner surface of the outer cylinder as the same manner of the inner cylinder. Five additional thermocouples were positioned at the mid-points of the gap distance of the annuli to measure the air temperatures. A digital temperature indicator of 0.1 °C resolution was used to record the temperatures. The electric power consumed by the heater was controlled by an altering variance unit of 1 kVA capacity. An ammeter of 0.01 Ampere resolution and a voltmeter of 0.1 volt resolution were used to measure the electric power consumed by the heater. The experimental work scans the effect of aspect ratio, orientations of the specimens (vertical, horizontal and inclined) and the angle of rotation of the major axis for horizontal and inclined orientations as shown in fig. 3., on the natural convection heat transfer in the annuli.

Table 1
Main dimensions of the test specimens

Dimensions in (mm)	Spec. No. I	Spec. No. II	Spec. No. III	Spec. No. IV
a_i	50	42.85	33.33	20
b_i	50	57.15	66.67	80
a_o	100	85.7	66.67	40
b_o	100	114.3	133.33	160
Aspect ratio $= \frac{a_i}{b_i} = \frac{a_o}{b_o}$	1.00	0.75	0.50	0.25

3. Experimental data discussion

The main objective of this paper is to provide an evidence about the parameters that create a stronger buoyancy-driven plume which results in higher heat transfer coefficient by natural convection in the elliptic annuli. In the present experimental work, the heat transfer by natural convection can be evaluated as follows, [12,13]:

$$Q_{\text{conv.}} = Q_{\text{total}} - Q_{\text{rad.}} - Q_{\text{cond.}} \ . \tag{1}$$

where: Q_{total} is the electrical power consumed by the heater. The heat transfer by radiation from inner surface to outer one and to air in the annulus can be found as follows:

$$Q_{\text{rad.}} = \left[\begin{array}{l} \left(\dfrac{\sigma P_i L\ (T_i^4 - T_o^4)}{1/\varepsilon_i + ((1-\varepsilon_o)/\varepsilon_o)\ P_i/P_o} \right) \\ + \left(\sigma P_i L\ \varepsilon_i\ (T_i^4 - T_a^4) \right) \end{array} \right] . \tag{2}$$

The heat transfer by conduction from the two ends of the inner cylinder can be found as follows:

$$Q_{\text{cond.}} = \frac{2\ P_i\ t\ (T_c - T_e)}{L / 2k_s} . \tag{3}$$

The average convective heat transfer coefficient, average Nusselt number and Rayliegh number can be found as follows:

$$\overline{h} = Q_{\text{conv.}} / P_i\ L\ (T_i - T_o) . \tag{4}$$

$$\overline{Nu} = \frac{\overline{h}\ \delta}{k}. \qquad (5)$$

The air properties in the above equations are evaluated at the mean temperature, [14,15], $[T_m = (T_i + T_o)/2]$.

$$Ra = \frac{g\ \beta\ (T_i - T_o)\ \delta^3}{\vartheta^2}\ Pr. \qquad (6)$$

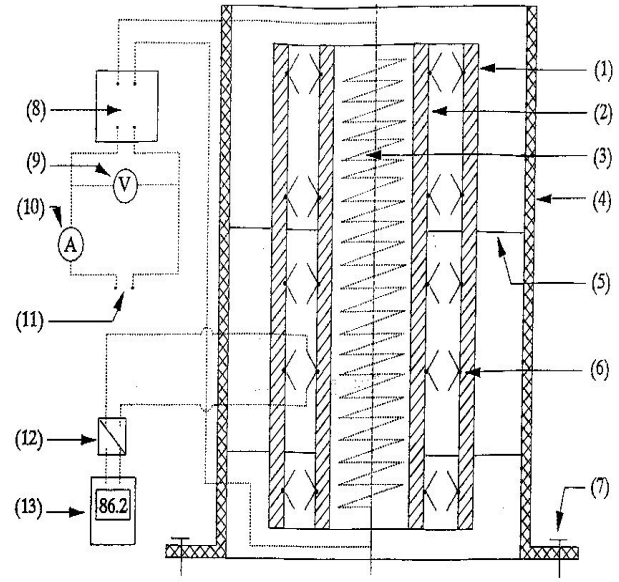

1- Outer cylinder
2- Inner cylinder
3- Electric heater
4- Glass room
5- Holding bar
6- K-type thermocouple
7-Adjusting screw
8- Variance
9- Voltmeter
10- Ammeter
11-AC-supply
12- Multi-switch
13- Temperature indicator

Fig. 1. Schematic of the experimental setup.

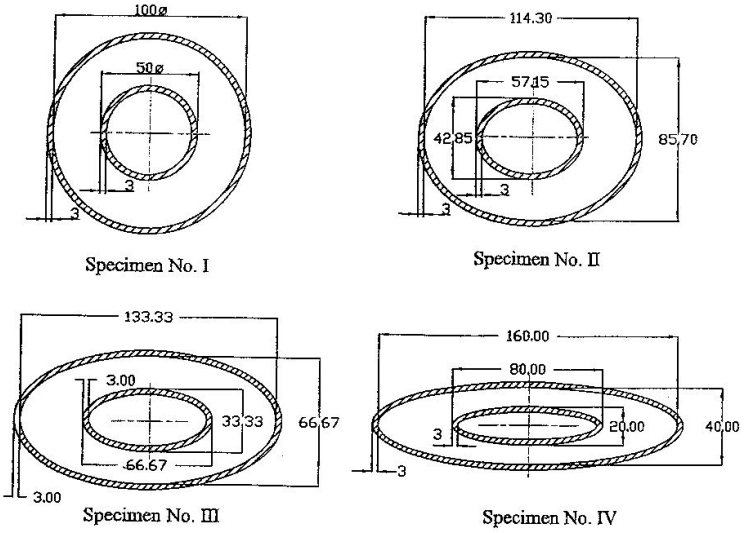

Fig. 2. Cross-sections of test specimens.

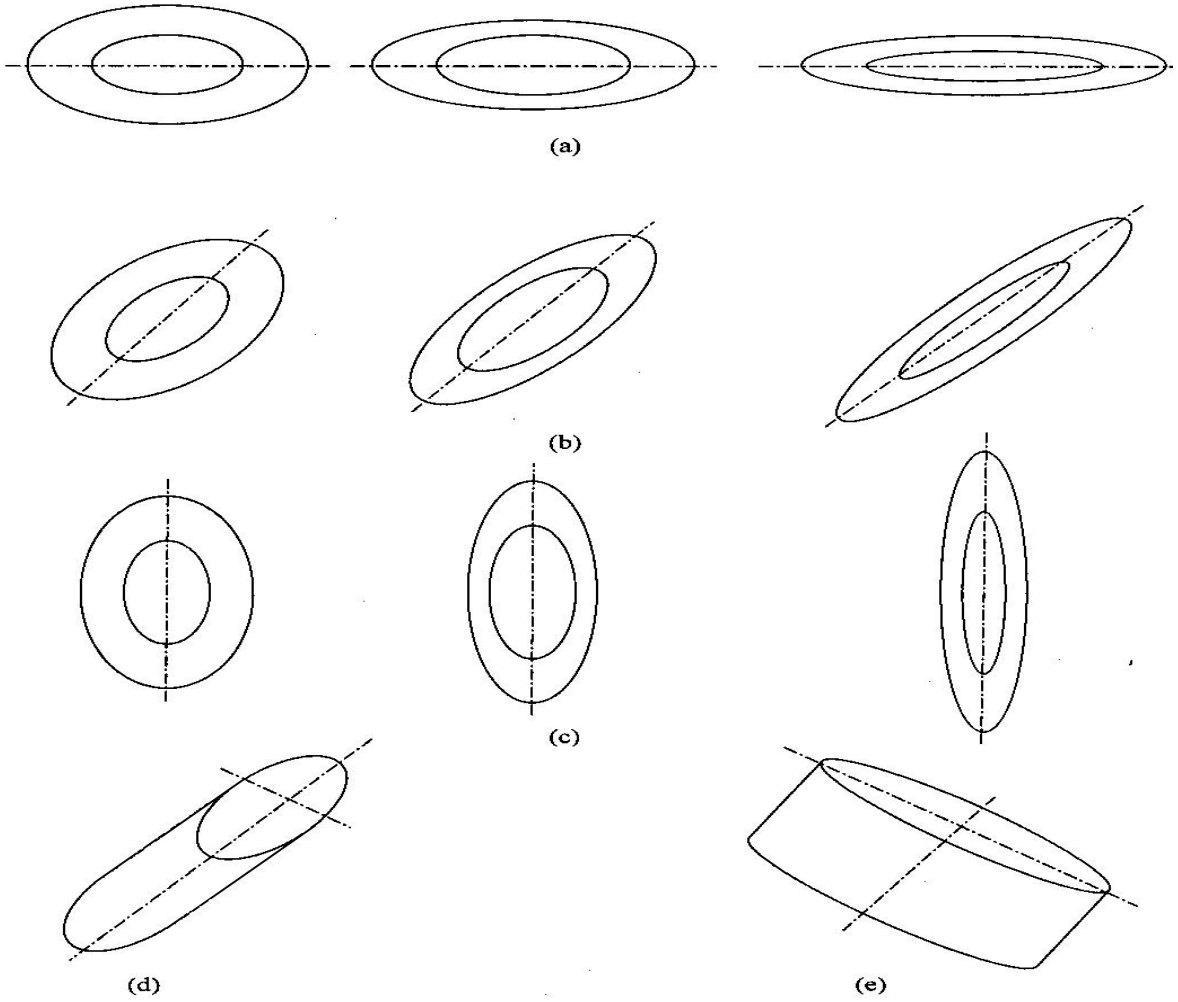

Fig. 3. Rotation of elliptic specimens No. II, III and IV whenever the specimens are oriented horizontally and inclined by an angle φ = 45 degree. a- horizontal (φ = 0 and ϕ = 0), b- horizontal (φ = 0 and ϕ = 45) degree), c- horizontal (φ = 0 and ϕ = 90 degree) d- Inclined (φ = 45 degree and ϕ = 0), and e- Inclined (φ = 45 degree and ϕ = 90 degree).

Fig. 4 shows Nusselt number versus Rayleigh number for the four test specimens when they were oriented vertically. The critical value of Rayleigh number, at which the change from conduction to convection heat transfer occurs, is 1400 for circular annulus with a diameter ratio, d_o/d_i=2.6, [4, 16]. In the present work, all tests were done for r1≥ 2000, therefore, the heat transfer in the annuli will fall in the convection regime. The figure shows that the heat transfer by natural convection in the circular annulus is relatively higher than that in the elliptic annuli. Also, the elliptic annulus having lower aspect ratio resulted in lower free convective heat transfer. The temperature gradient inside the annulus causes an upward velocity of the light air near the inner hot surface. While, the heavy air near the cold outer surface moves downward. The opposite light and heavy air movements create a complete circulation pattern, [17, 18]. The three elliptic annuli are having lower cross-section areas than that of the circular annulus. The reduction in the cross-section area causes an increase in the circulation of the air inside the elliptic annuli which reduces the upward buoyancy-driven plume and consequently the free convective heat transfer reduces.

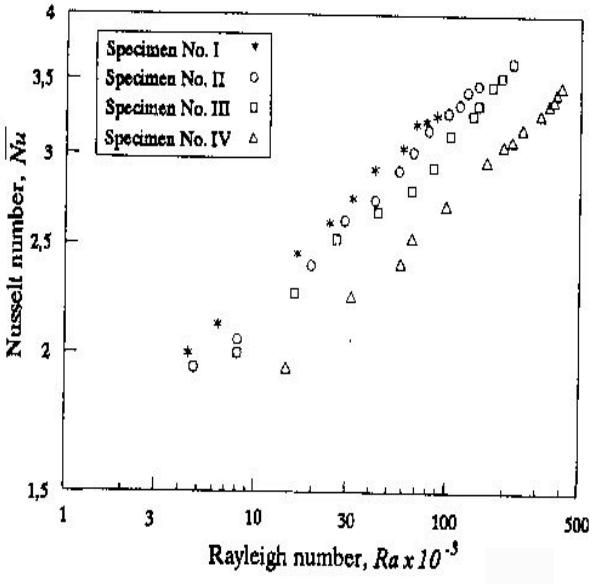

Fig. 4. Nusselt number vs Rayleigh number for the four specimens for vertical orientation.

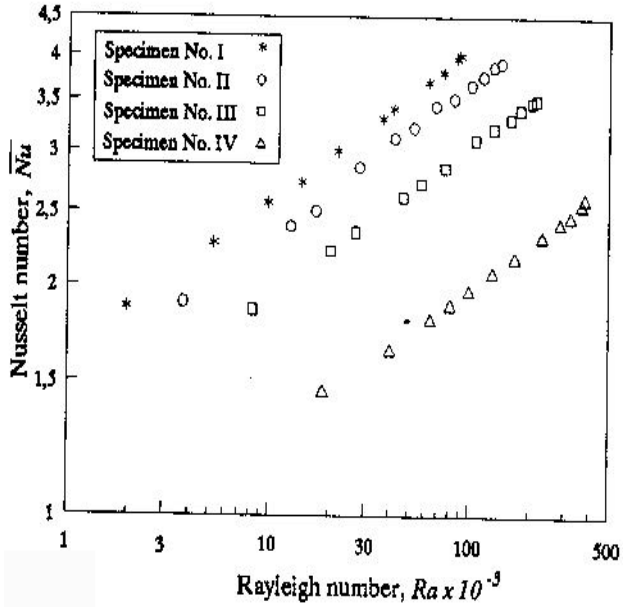

Fig. 5. Nusselt number vs Rayleigh number for the four specimens for horizontical orientation.

Referring to fig. 5, the same tendency of fig. 4 is even observed. Moreover, it is noted more reduction in the free convective heat transfer in the elliptic annuli than that of the circular annulus for horizontal orientation of the specimens. Referring to case (a) of fig. 3, the horizontal orientation of the specimens with major axes horizontal resists the upward buoyant-driven plume. The increase in the major axis length of the internal ellipse increases the resistance against the air plume. As a consequence, an intense reduction in the free convective heat transfer was noted for elliptic annuli having lower aspect ratio rather than the circular one. Fig. 6 shows that the

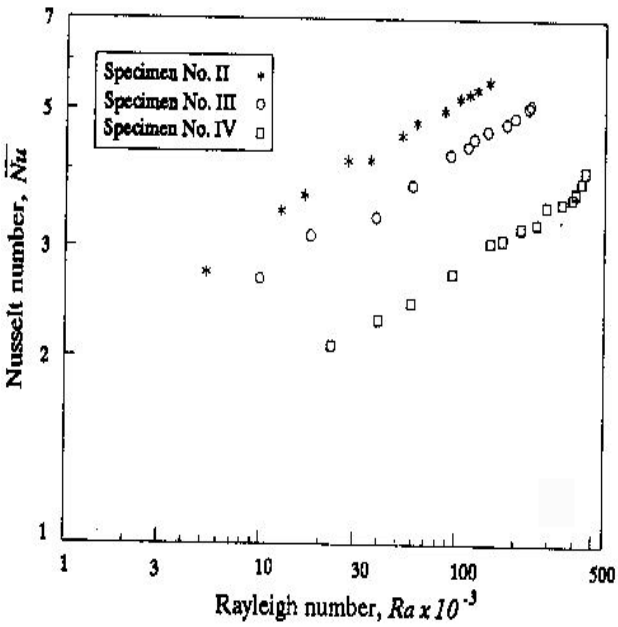

Fig. 6. Nusselt number vs Rayleigh number for the four specimens for horizontical orientation.

reduction in the free convective heat transfer in the elliptic annuli is reduced as the major axis of the elliptic annuli rotates by an angle ϕ = 45 degree, the orientation of case (b) of fig. 3. The rotation of major axis of elliptic annuli by an angle ϕ = 90 degree whenever the specimens were laid horizontally, case (c) of fig. 3, results in more increase in the free convective heat transfer in the elliptic annuli rather than the circular annulus. Moreover, the elliptic annuli having lower as ratio show higher values of Nusselt number at the same Rayleigh number as shown in fig. 7. This is referred to the reduction in the resistance against upward air plume which is resulted from the reduction in length of the minor axis. Thus, one can say, the natural convective heat transfer in the elliptic annuli increases as the aspect ratio decreases for horizontal orientation with major axis is vertical.

The effect of inclination of the specimens was also clarified. The four specimens were tested experimentally when the symmetrical axis was inclined by an angle φ = 45 degree to horizontal plane, in two different situations, cases (d and e) of fig. 3. Case (d); φ = 45 degree and minor axis of the elliptic section makes an angle 45 degree with the horizontal plane while, the major axis is parallel to the horizontal plane, i.e. the specimen is inclined without rotation, i.e. ϕ = 45 degree. Case (e); φ = 45 degree and major axis of the elliptic section makes an angle 45 degree with the horizontal plane while, the minor axis is parallel to the horizontal plane, i.e. the specimen is inclined and rotates by a right angle, i.e. ϕ = 90 degree. Fig. 8 shows that the inclined circular annuli give higher free convective heat transfer rates rather than the elliptic ones without rotation. Moreover, the reduction in the aspect ratio of the elliptic annuli results in more reduction in the free convective heat transfer rates. This is because the increase in the projected area of the inner elliptic cylinder which creates more resistance for the upward air plume. The reverse of the previous result in fig. 8. is clear in fig. 9, where the elliptic annuli having the smallest aspect ratio show higher free convective heat transfer rather than the circular ones. This is referred to the reduction in the projected area of the inner elliptic cylinder which reduces the resistance of the upward air plume flow.

In the following, the effect of orientation on the experimental results for each specimen alone will be clarified. Fig. 10 shows that the inclination of the circular annulus results in higher free convective heat transfer rather than the horizontal orientation. Also, the horizontal orientation of the circular annulus shows more increase in Nusselt number at the same Rayleigh number rather than the vertical orientation. Fig. 11 shows the experimental results of the elliptic annulus having an aspect ratio = 0.75 in different orientation modes. The figure clarifies that the inclination of the specimen with a rotation by a right angle as well as the horizontal orientation with a rotation by a 45 degree are having higher heat transfer rates rather than the different orientation modes. Figs. 12 and 13 show that either inclination with a rotation by a right angle or horizontal orientation with a rotation by a right angle of both specimens No. III and IV are having higher heat transfer rates rather than the different orientation modes. Figs. 12

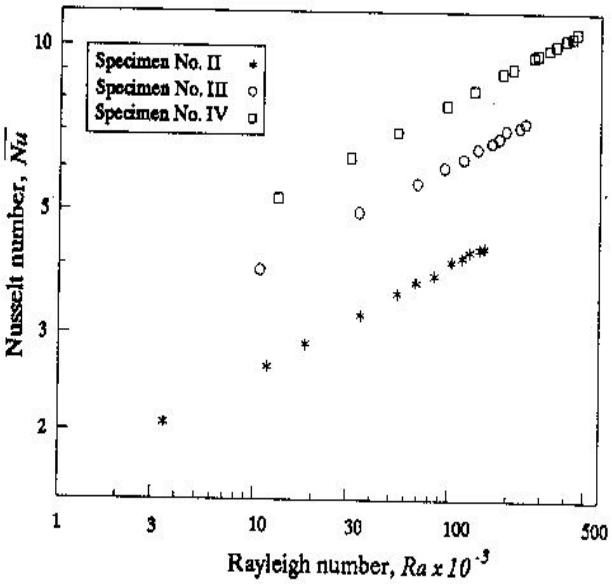

Fig. 7. Nusselt number vs Rayleigh number for the specimens in horizontal orientation and ϕ= 90 degree.

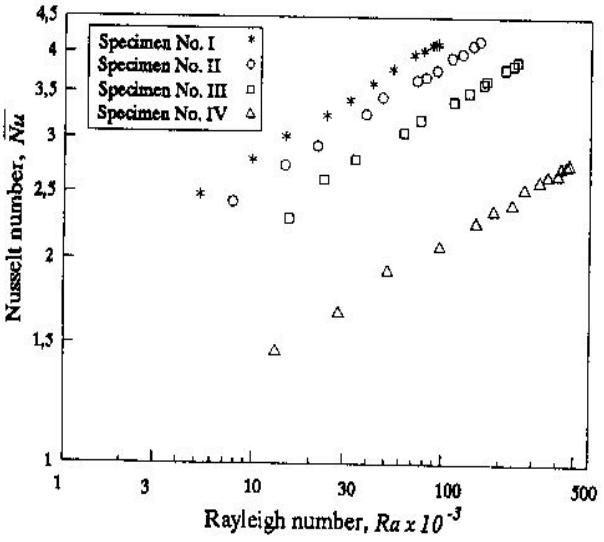

Fig. 8. Nusselt number vs Rayleigh number for the four specimens for (φ= 45 degree and ϕ = 0).

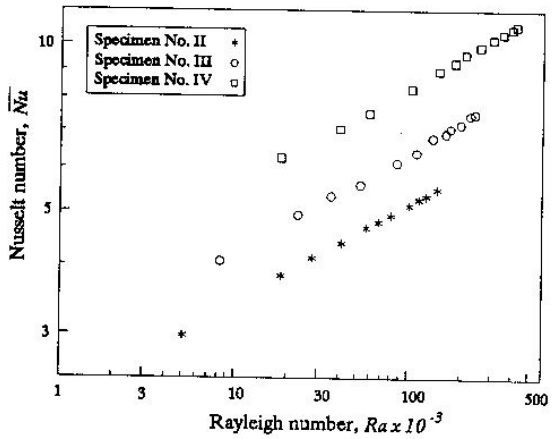

Fig. 9. Nusselt number vs Rayleigh number for the specimens for (φ= 45 degree and ϕ = 90 degree).

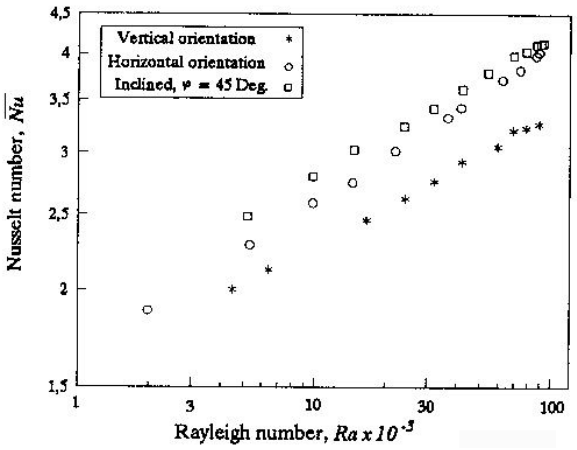

Fig. 10. Nusselt number vs Rayleigh number for the specimens No. I for different orientations.

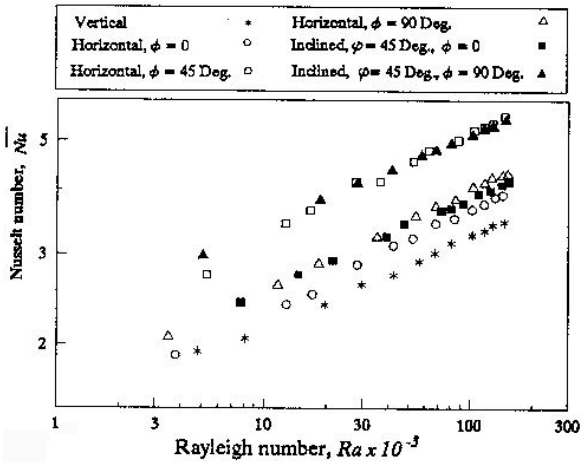

Fig. 11. Nusselt number vs Rayleigh number for the specimens No. II for different orientations.

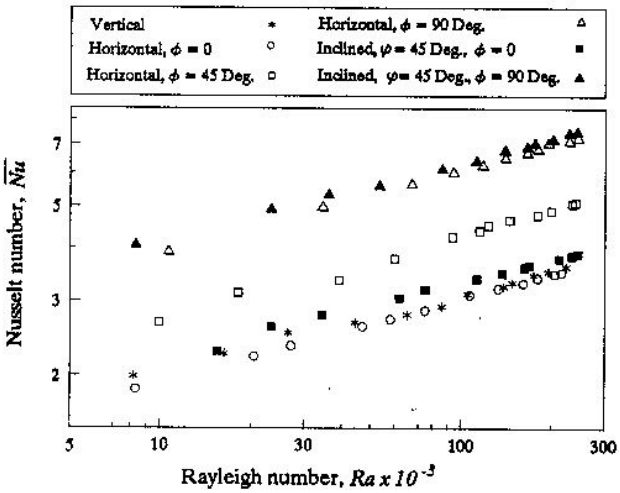

Fig. 12. Nusselt number vs Rayleigh number for the specimens No. III for different orientations.

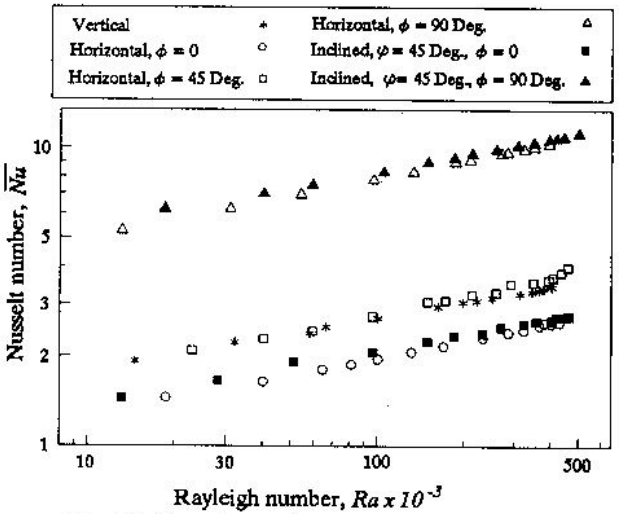

Fig. 13. Nusselt number vs Rayleigh number for the specimens No. IV for different orientations.

The experimental results were fitted to determine empirical correlations among Nusselt number, Rayleigh number and aspect ratio for , as follows:

$$\overline{Nu} = C\, Ra^{n} \left(\frac{a}{b}\right)^{m} . \qquad (7)$$

Where; the constants *C, n* and *m* are tabulated as follows.

4. Mathematical modeling and numerical solution

The natural convection heat transfer between two horizontal concentric cylinders results in a buoyancy-driven flow in a vertical r-θ plane. The space coordinates are r, measured from the center of the cylinder and, θ, measured anti-clockwise from the downward vertical symmetry line. The two-dimensional governing equations were summarized as follows under the following assumptions, [19]:

a) The flow is laminar;
b) The axis of the cylinder is infinite in length;
c) The fluid is incompressible except the Boussinesq approximation for the density in the buoyancy term of the momentum equation;
d) Steady;
e) The viscous dissipation is negligible in the energy equation.

Continuity equation:

$$\frac{\partial v_r}{\partial r}+\frac{v_r}{r}+\frac{1}{r}\frac{\partial v_\theta}{\partial \theta}=0\,, \tag{8}$$

r-momentum equation:

$$\rho\left(v_r\frac{\partial v_r}{\partial r}+\frac{v_\theta}{r}\frac{\partial v_r}{\partial \theta}-\frac{v_\theta^2}{r}\right)=-\frac{\partial p}{\partial r} +\mu\left[\begin{array}{l}\dfrac{\partial}{\partial r}\left(\dfrac{1}{r}\dfrac{\partial}{\partial r}(v_r r)\right)+\\ \dfrac{1}{r^2}\left(\dfrac{\partial^2 v_r}{\partial \theta^2}\right)-\dfrac{2}{r^2}\dfrac{\partial v_\theta}{\partial \theta}\end{array}\right]+F_r\,, \tag{9}$$

Table 2
Constants of empirical correlations

	C	0.5221
Vertical orientation;	n	0.1573
	m	0.1719
Horizontal orientation; ϕ = 0.	C	0.5570
	n	0.1795
	m	0.4901
Horizontal orientation; ϕ = 45 Deg.	C	0.6209
	n	0.1845
	m	0.4007
Horizontal orientation; ϕ = 90 Deg.	C	0.6452
	n	0.1970
	m	0.3261
Inclined orientation; φ = 45 Deg., ϕ = 0.	C	0.5592
	n	0.1780
	m	0.4932
Inclined orientation; φ = 45 Deg., ϕ = 90 Deg.	C	0.5304
	n	0.1830
	m	-0.4842

θ-momentum equation:

$$\rho\left(v_r\frac{\partial v_\theta}{\partial r}+\frac{v_\theta}{r}\frac{\partial v_\theta}{\partial \theta}-\frac{v_r v_\theta}{r}\right)=-\frac{1}{r}\frac{\partial p}{\partial \theta} +\mu\left[\begin{array}{l}\dfrac{\partial}{\partial r}\left(\dfrac{1}{r}\dfrac{\partial}{\partial r}(v_\theta r)\right)+\\ \dfrac{1}{r^2}\left(\dfrac{\partial^2 v_\theta}{\partial \theta^2}\right)+\dfrac{2}{r^2}\dfrac{\partial v_r}{\partial \theta}\end{array}\right]+F_\theta\,. \tag{10}$$

Energy equation:

$$\left(v_r\frac{\partial T}{\partial r}+\frac{v_\theta}{r}\frac{\partial T}{\partial \theta}\right)= \alpha\left[\left(\frac{1}{r}\frac{\partial}{\partial r}(r)\frac{\partial T}{\partial r}\right)+\frac{1}{r^2}\left(\frac{\partial^2 T}{\partial \theta^2}\right)\right]\,. \tag{11}$$

The buoyancy forces in r and θ directions are written as:

$$F_r=\rho_\infty g\beta(T-T_\infty)\sin\theta\,. \tag{12}$$

$$F_r=\rho_\infty g\beta(T-T_\infty)\sin\theta\,. \tag{13}$$

The boundary conditions for this model as shown in fig. 14 are:
- At the surface of the inner cylinder;

($r = r_i$; $0 \le \theta \le \pi$)

$$v_r = v_\theta = 0\,. \tag{14}$$

$$\frac{\partial T}{\partial r}=\text{constant} \tag{15}$$

- At the surface of the outer cylinder;

($r = r_i$; $0 \le \theta \le \pi$)

$$v_r = v_\theta = 0\,. \tag{16}$$

$$] T = T_\infty\,. \tag{17}$$

- At the symmetry line;

($r_i \le r \le r_o$ *and* $\theta = 0$ and π)

$$\frac{\partial v_\theta}{\partial \theta}=\frac{\partial T}{\partial \theta}=0\,. \tag{18}$$

The governing equations were solved using FLUENT-6-CFD code, [20]. The package was used to predict the air properties at the same conditions of the experimental work. It provides also a complete information about streamlines contours and isotherm contours that can not be obtained experimentally. In order to verify the experimental results, a comparison between the predicted results and corresponding experimental results for the four specimens at the same conditions was done. Fig. 15 shows that the average deviation of the numerical solution from experimental data is about 7%. This is referred to measurement errors, averaging surfaces temperatures of test specimens and numerical model assumptions. For this reason, the CFD model was used to predict the effect of the diameter ratio, d_o/di for the circular annulus which was not done experimentally. Fig. 16 shows that the increase in the diameter ratio results in an increase in free convective heat transfer in the circular annuli. Fig. 17 shows some of the predicted isotherm contours. The figure shows the temperature distribution inside the annulus and how it varies from the inner surface to the outer one. The isotherm contours take a so-called upward eccentric circles shape and the eccentricity reduces as the contours come close to outer surface.

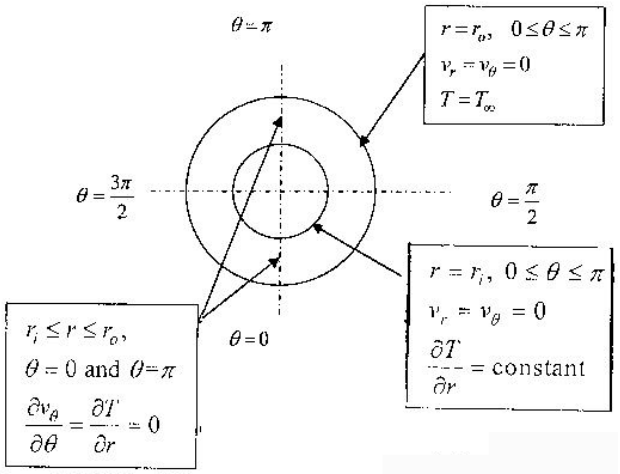

Fig. 14. Boundary conditions for the concentric horizontal cylinders.

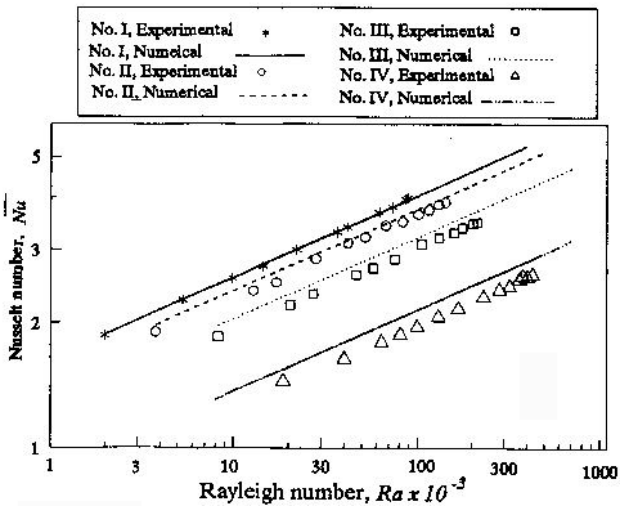

Fig. 15. Comparison between predicted results and experimental results for specimens in horizontal orientation and $\phi = 0$.

5. Comparison among present work and previous works

In this section, a comparison between the experimental results of the present work and the experimental results of the previous work will be discussed. Another comparison between the numerical predictions of the present work and pre-correlated numerical data in the literature will be clarified. The conduction limit at which the change from conduction to convection heat transfer occurs, is 1400 for circular annulus with a diameter ratio, d_o/d_i = 2.6, [4, 16]. In the present work, all tests were done for Ra $\geq$ 2000, The conduction limit for a diameter ratio of 2.0 is as follows:

$$\overline{Nu}_{cond} = \frac{1}{\ln\left[\frac{d_o}{d_i}\right]} = \frac{1}{\ln 2} = 1.4427 \qquad (19)$$

This limit is clear in fig. 18. Referring to this figure, the experimental results of the present work of the circular annulus having a diameter ratio of 2 in horizontal orientation were compared with the experimental results of a circular annulus in horizontal orientation and having a diameter ratio of 2.57, [9]. The comparison shows that the results of the previous work are higher than the results of the present work which is referred to the increase in the diameter ratio of the previous work. Also, the natural convection heat

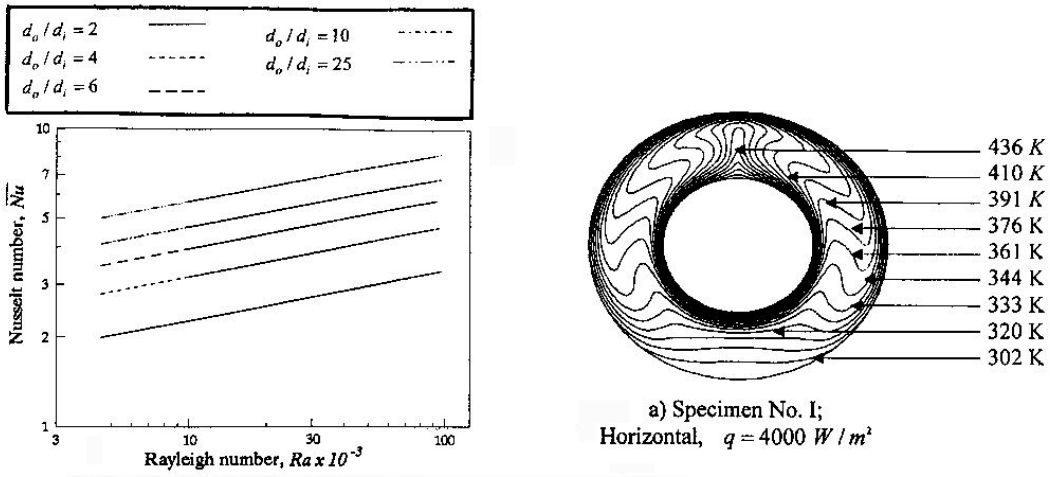

Fig. 16. Effect of diameter ratio on Ra-Nu results for specimen No. I for horizontal orientation

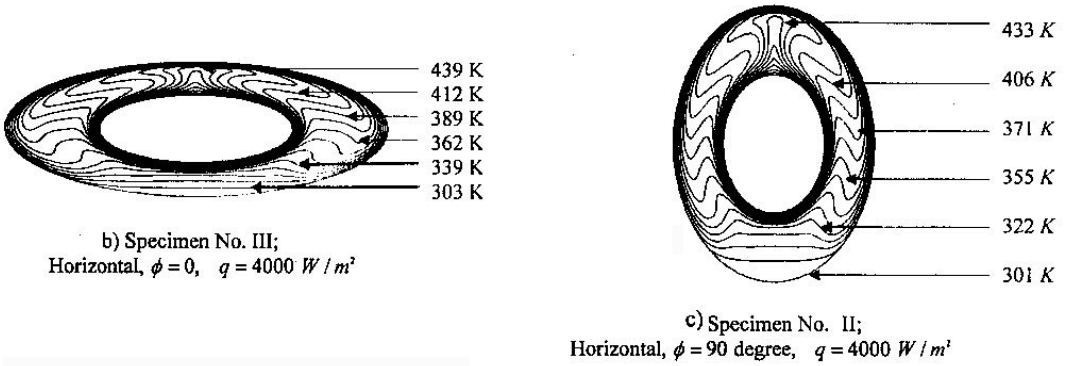

Fig. 17. Some of the predicted isotherms.

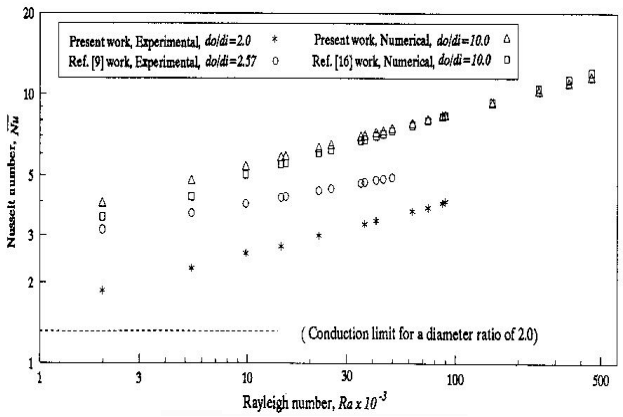

Fig. 18. Compression among the results of the present work and previous work.

transfer in a circular annulus having a diameter ratio of 10 in horizontal orientation was studied numerically, [16]. The CFD model of the present work was used to solve this problem at its conditions and the predictions from the present work were compared with the previous predictions, as shown in fig. 18. A fairly good agreement between the two predictions was established.

6. Conclusions

Natural convection heat transfer in elliptic annuli with different aspect ratio was studied experimentally and numerically. The experimental work was conducted with the clarification of the effect of aspect ratio and

orientation modes that create stronger buoyant driven plume. The experimental data were fitted to deduce empirical correlations. A mathematical model was formulated in $r-\theta$ coordinates for the space between a pair of concentric horizontal cylinders having either circular cross sections or elliptic ones. The model was solved numerically using the FLUENT CFD package. The main conclusions from the present work can be summarized as follows:

1- Natural convective heat transfer in concentric elliptic annuli increases by about 40 % rather than the circular annuli having the same perimeter as the aspect ratio decreases to 0.25 in the horizontal orientation and the major axis is vertical.

2- The inclination of the elliptic annuli having small aspect ratio with minor axis parallel to horizontal plane improves the free convective heat transfer in the annuli.

3- In both horizontal and inclination situations of the elliptic annuli with rotating the major axis by a right angle; the reduction in the aspect ratio results in higher free convective heat transfer rates in the annuli.

4- The CFD model shows that the increase in the diameter ratio of the elliptic annulus increases the free convective heat transfer rates. Also, the CFD model can be considered a suitable simulator tool for solving the free convective heat transfer characteristics in the elliptic annuli.

5- In vertical orientation, the reduction in the aspect ratio reduces the free convective heat transfer rates.

6- Comparisons between experimental and numerical results of the present work, as well as, the comparison among the results of the present work and those in the literature show fairly good agreement.

Nomenclature

a Minor axis length m,
b Major axis length m,
d Diameter m,
F Force N,
g Gravity acceleration m/s^2
h Heat transfer coefficient W/m^2.K,
k Thermal conductivity W/m.K,
L Length m,
Nu Nusselt number,
P Perimeter m,
Pr Prandtl number,
p Pressure Pa.,
$\dot{Q}$ Heat transfer rate W,
q Heat flux W/m^2,
Ra Rayleigh number,
r Radial coordinate m,
T Temperature K,
Δt Temperature difference = T_i-T_o,
t Cylinder wall thickness m,
v Velocity m/s,
α Thermal diffusivity m^2/s,
β Volume coefficient of expansion K^{-1},
δ Gap width = $(b_o-b_i)/2$ m,
ε Surface emissivity,
ϕ Rotation of major axis Degree,
φ Inclination angle Degree,
θ Angular coordinate Radiant,
ϑ Kinematical viscosity m^2/s,
μ Dynamic viscosity Pa.s,
ρ Density kg / m^3, and
σ Stefan-Boltzman constant W/m^2 K^4.

Subscripts

A Air
i Inner cylinder
s Solid
c Mid-section
o Outer cylinder
θ Tangential direction
e End-section
r Radial direction
∞ Reference value

References

[1] Y. Rao, Y. Miki, K. Fukuda, Y. Takata, and S. Hasegawa, "Flow Pattern of Natural Convection in Horizontal Cylindrical Annuli", Int. J. Heat Mass Transfer, Vol. 28 (3), pp. 705-714 (1985).

[2] E.H. Bishop, Heat Transfer by Natural Convection of Helium Between Horizontal Isothermal Concentric Cylinders at Cryogenic Temperature,

Journal of Heat Transfer, Vol. 110, pp. 109-115 (1988).

[3] A. Castrejon and D.B. Spalding, "An Experimental and Theoretical Study of Transient Free Convection Flow Between Horizontal Concentric Cylinders", Int. J. Heat Mass Transfer, Vol. 31 (2), pp. 273-284 (1988).

[4] R. Kumar and M. Keyhani, "Flow Visualization Studies of Natural Convective Flow in a Horizontal Cylindrical Annulus", Journal of Heat Transfer, Vol. 112, pp. 784-787 (1990).

[5] S.M. Saboya and F.E.M. Saboya, "Experiments on Elliptic Sections in One-and Two-Row Arrangements of Plate Fin and Tube Heat Exchangers", Experimental Thermal and Fluid Science Vol. 24, pp. 67-75 (2001).

[6] Shu, H. Xue and Y.D. Zhu, "Numerical Study of Natural Convection in an Eccentric Annulus Between a Square Outer Cylinder and a Circular Inner Cylinder Using DQ Method", Int. J. of Heat and Mass Transfer, Vol. 44, pp. 3321-3333 (2001).

[7] H.A. Eball, M.B. Hassan, "Mixed Convection from an Elliptic Tube Placed in a Fluctuating Free Stream", Int. J. of Engineering Science, Vol. 39, pp. 669-693 (2001).

[8] E.A.A., El-Kady, "Enhancement of Heat Transfer by Natural Convection from Horizontal Cylinders by Using Shrouding Strips", Proceedings of the 10th Int. AMME Conference, MTC, Cairo, Egypt (2002).

[9] F.A. Hamad, and M.K Khan, "Natural Convection Heat Transfer in Horizontal and Inclined Annuli of Different Diameter Ratios", Energy Convers Mgmt Vol. 39 (8), pp. 797-807 (1998).

[10] JSEDM, WIRECUT EDM, Operation Instruction, Jiann Sheng Machinery & Electric Industrial Co., LTD.

[11] J.P. Holman, Experimental Methods for Engineers, McGraw-Hill International Edition, Seventh Edition, New York, USA (2001).

[12] J.P. Holman, Heat Transfer, McGraw-Hill Co., Ninth Edition, New York, USA (2002).

[13] F.P. Incropera and D.P. Dewitt, Fundamentals of Heat and Mass Transfer, John Wiley & Sons, Inc., Fourth Edition, New York, USA (1996).

[14] I.H. Shames, Mechanics of Fluids, McGraw-Hill Inc., Third Edition, New York, USA (1992).

[15] Y.A. Cengel, and M.A. Boles, Thermodynamics: An Engineering Approach, McGraw-Hill Co., Third Edition, NY. USA (1998).

[16] R. Kumar, "Study of Natural Convection in Horizontal annuli", Int. J. Heat Mass Transfer, Vol. 31 (6), pp. 1137-1148 (1988).

[17] E. Buyruk, H. Barrow and I. Owen, "Heat Transfer in Laminar Flow in a Concentric Annulus with Peripherally Varying Heat Transfer", Int. J. of Heat and Mass Transfer, Vol. 42, pp. 487-496 (1999).

[18] D. Naylor, H.M. Badr and J. D. Tarasuk, "Experimental and Numerical Study of Natural Convection Between Two Eccentric Tubes", Int. J. Heat Mass Transfer, Vol. 32 (1), pp. 171-181 (1989).

[19] H.K. Versteeg, and W. Malalasekera, An Introduction to Computation Fluid Dynamics, The Finite Volume Method, John Wiley, Sons Inc., 605 Third Avenue, New York, USA (1995).

[20] Fluent, Fluent user's guide, Lebanon, Fluent Inc., USA (2000).

Received September 16, 2004
Accepted December 7, 2004